

Modeling the feedback between aerosol and boundary layer processes: a case study in Beijing, China

Yucong Miao¹ · Shuhua Liu¹ · Yijia Zheng¹ · Shu Wang¹

Received: 26 June 2015 / Accepted: 6 October 2015 / Published online: 21 October 2015
© Springer-Verlag Berlin Heidelberg 2015

Abstract Rapid development has led to frequent haze in Beijing. With mountains and sea surrounding Beijing, the pollution is found to be influenced by the mountain-plain breeze and sea-land breeze in complex ways. Meanwhile, the presence of aerosols may affect the surface energy balance and impact these boundary layer (BL) processes. The effects of BL processes on aerosol pollution and the feedback between aerosol and BL processes are not yet clearly understood. Thus, the Weather Research and Forecasting model coupled with Chemistry (WRF-Chem) is used to investigate the possible effects and feedbacks during a haze episode on 23 September 2011. Influenced by the onshore prevailing wind, sea-breeze, and upslope breeze, about 45 % of surface particulate matter ($PM_{2.5}$) in Beijing are found to be contributed by its neighbor cities through regional transport. In the afternoon, the development of upslope breeze suppresses the growth of BL in Beijing by imposing a relatively low thermal stable layer above the BL, which exacerbates the pollution. Two kinds of feedback during the daytime are revealed as follows: (1) as the aerosols absorb and scatter the solar radiation, the surface net radiation and sensible heat flux are decreased, while BL temperature is increased, resulting in a more stable and shallower BL, which leads to a higher surface $PM_{2.5}$ concentration in the morning and (2) in the afternoon, as the

presence of aerosols increases the BL temperature over plains, the upslope breeze is weakened, and the boundary layer height (BLH) over Beijing is heightened, resulting in the decrease of the surface $PM_{2.5}$ concentration there.

Keywords WRF-Chem · Boundary layer · Mountain-plain breeze · Sea-land breeze · Aerosol pollution

Introduction

Beijing, located on the northeastern coast of China, is the capital and center of politics, culture, and economics of China, covering an area of 16,000 km². Due to the rapid economic and industrial development in the past three decades, Beijing has become an impressive modern city with more than 20 million inhabitants. Simultaneously, such tremendous development has also resulted in frequent haze there (He et al. 2001; Xia et al. 2007; Chan and Yao 2008; Huang et al. 2014; Li et al. 2014; Quan et al. 2014; Fu et al. 2014; Che et al. 2015; Han et al. 2015). The annual average particulate matter ($PM_{2.5}$) concentration from 2008 to 2014 in Beijing varied between 90.8 and 104.7 $\mu\text{g m}^{-3}$, and the highest hourly average $PM_{2.5}$ concentration recorded was 994 $\mu\text{g m}^{-3}$ at midnight on 23 January 2012 (San Martini et al. 2015).

The atmospheric aerosols can absorb and scatter the solar and thermal radiation, which is known as the direct effect (Atwater 1970; Coakley et al. 1983; Sokolik and Toon 1996; Yu et al. 2006). On the other hand, the aerosols can act as cloud condensation nuclei (CCN) to change the microphysical and optical properties of cloud droplets, which is the indirect effect (Albrecht 1989; Rosenfeld and Lensky 1998). These effects of aerosol lead to the decrease of the solar radiation reaching the surface (Liu et al. 2007; Xia et al. 2007; Saha et al. 2008; Zhuang et al. 2010; Huang et al. 2015), and change

Responsible editor: Gerhard Lammel

✉ Yucong Miao
miaoyucong@yeah.net

✉ Shuhua Liu
lshuhua@pku.edu.cn

¹ Department of Atmospheric and Oceanic Sciences, School of Physics, Peking University, No. 209 Chenfu Road, Haidian District, Beijing 100871, China

the atmospheric structure (Li et al. 2007; Gao et al. 2015) and precipitation process (Ramanathan et al. 2001). Based on the long-term measurements of a suburban site around Beijing, Li et al. (2007) and Xia et al. (2007) reported that the annual 24-h mean aerosol direct effect was $\sim 25 \text{ W m}^{-2}$. During the heavy pollution episode, Liu et al. (2007) observed that the instantaneous aerosol direct effect could reach as high as 350 W m^{-2} over northern China, and 300 W m^{-2} of which was absorbed by the atmosphere, resulting in a more stable atmosphere. In a field experiment in Tianjin from 9 to 30 September 2010, Quan et al. (2013) found that the development of the boundary layer (BL) during the aerosol pollution episode was suppressed due to the decreases of surface solar radiation and sensible heat flux. Based on the modeling studies, Gao et al. (2015) also demonstrated that aerosol led to a significant negative radiative forcing on the surface and imposed a large positive radiative forcing in the atmosphere. These aerosol effects not only influence the surface meteorological variables (Qian et al. 2003; Liu et al. 2010), but also in turn increase the surface aerosol concentrations by lowering the boundary layer height (BLH) and enhancing the atmosphere stability (Wang et al. 2013; Gao et al. 2015).

The city of Beijing lies on flat land that opens to the east and south, and is surrounded by the Yan and Taihang Mountains in the north and west (Fig. 1a), about 150 km inland from the Bohai Sea via Tianjin in the southeast (Fig. 1b). Such topography affects the BL processes there in complex ways (Chen et al. 2009; Liu et al. 2009; Sun et al. 2013; Hu et al. 2014; Dou et al. 2015; Miao et al. 2015a, b). Under favorable synoptic conditions, the local thermally induced mountain-plain breeze develops frequently in Beijing (Chen et al. 2009; Hu et al. 2014; Dou et al. 2015; Miao et al. 2015a) and may play an important role in modulating the local air quality (Chen et al. 2009; Hu et al. 2014; Miao et al. 2015b). Based on the airplane measurements over Beijing, Chen et al. (2009) reported that an elevated pollution layer was formed by the daytime upslope breeze on 18 August 2007. Hu et al. (2014) reported that the development of upslope breeze suppressed the growth of BL in Beijing and exacerbated the ozone pollution on 16 August 2013. In addition to the mountain-plain breeze, the sea-breeze (Liu et al. 2009; Sun et al. 2013; Zhang et al. 2013; Miao et al. 2015a) that developed over the coastal area of Bohai Sea may penetrate inland to Beijing (Liu et al. 2009; Zhang et al. 2013), and trap the pollutants in Beijing and its neighbor cities (Sun et al. 2013). Although the effect of BL processes on the air pollution in Beijing has been reported by a few case studies (Chen et al. 2009; Sun et al. 2013; Hu et al. 2014), a few questions about the BL processes still remain unclear, including (1) how the BL processes affect the horizontal distribution of the aerosols emitted from Beijing and its neighbor cities and (2) how the BL processes impact the vertical distribution of aerosols during the daytime. One objective of the present study is to

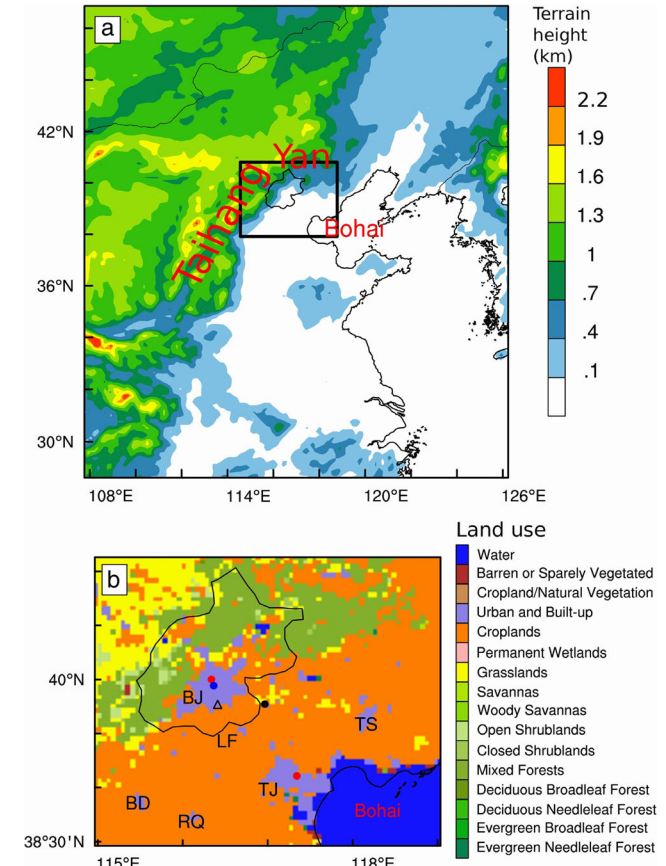


Fig. 1 **a** Map of model domains and terrain height (km) in domain 1. **b** Land use distribution in domain 2. The two red dots indicate the locations of two surface meteorological stations, and the PM_{2.5} monitoring station is marked by the blue dot, and the AERONET Xianghe site is marked by the black dot. The location of Nanjiao sounding site is marked by the triangle. The domain 2 covers Beijing (BJ) and Tianjin (TJ), and four industrious cities of Hebei province, which are Baoding (BD), Tangshan (TS), Langfang (LF), and Renqiu (RQ)

further unravel the possible effect of BL processes on aerosol pollution in Beijing.

The evolution of local, thermally induced atmospheric circulations are directly controlled by the surface net radiation and sensible heat flux (Miller 2003; Crosman and Horel 2010; Serafin and Zardi 2010). Therefore, during the aerosol pollution episodes, the decrease of solar radiation reaching surface not only simply leads to a relatively shallow BL (Quan et al. 2013; Gao et al. 2015), but also may modulate the developments of mountain-plain breeze and land-sea breeze. How the aerosol radiation effect influences these local atmospheric circulations, and then in turn modulates the local pollution level, has been rarely studied. Most of previous studies have merely focused on how the aerosol radiation effect influences the regular surface meteorological variables and the BLH (Li et al. 2007; Quan et al. 2013; Gao et al. 2015; Zhang et al. 2015a), ignoring the feedback between aerosol and the local atmospheric circulations.

In this study, to further understand the effects of BL processes on aerosol pollution in Beijing and to investigate the possible feedback between aerosol and BL processes, a three-dimensional chemical transport model is used, and the first day of a haze episode (Liu et al. 2013), which occurred on 23–27 September 2011 has been selected. The remainder of this paper is organized as follows: in “**Methodology**” section, the model and the design of numerical experiments are described. In “**Results**” the effects of BL processes on the aerosol pollution are first presented, and then the feedback between aerosol and BL processes is discussed. Finally, the main findings of this study are summarized in “**Conclusions**.”

Methodology

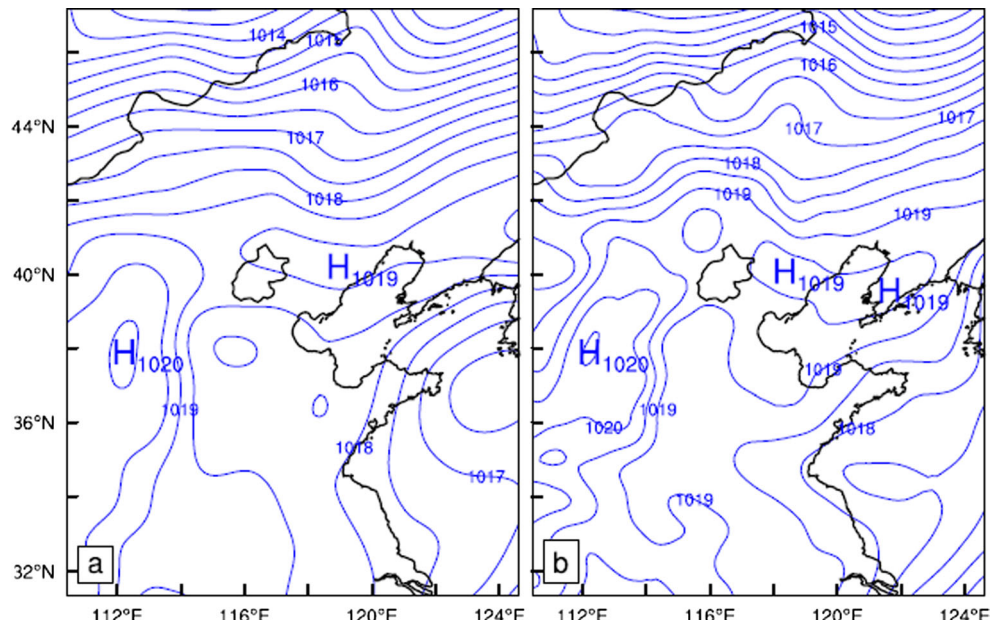
Design of numerical experiments

In this study, the Weather Research and Forecasting model coupled with Chemistry (WRF-Chem, version 3.6) is used, which simulates transport, mixing, and chemical transportation of gases and aerosols simultaneously with meteorological fields (Grell et al. 2005). Two one-way nested domains with horizontal grid spacing of 13.5 and 4.5 km (Fig. 1a) are used with the 1 km×1 km MODIS 2010 land use dataset (Justice et al. 2002) (Fig. 1b). As depicted in Fig. 1b, domain 2 covers the Beijing-Tianjin-Hebei (BTH) region, including the two mega cities (i.e., Beijing and Tianjin) and major industrious cities of Hebei province (i.e., Tangshan, Baoding, Langfang, and Reqiu). In the vertical dimension, 48 vertical layers are set from the surface to the 100-hPa level, and 21 layers of which are set below 2 km above ground level (AGL) to resolve the processes within BL. The physics parameterization schemes

used in this study include the Lin microphysics scheme (Lin et al. 1983), the Rapid Radiative Transfer Model for General circulation models (RRTMG) longwave/shortwave scheme (Iacono et al. 2008) with the aerosol direct effect, the Grell-Freita cumulus scheme (Grell and Freitas 2014), the Yonsei University (YSU) BL scheme (Hong et al. 2006), and the Noah land surface scheme (Chen and Dudhia 2001) with a single urban canopy model (Kusaka et al. 2001). In the YSU BL scheme, the BLH is diagnosed using the Richardson number method (Hong et al. 2006).

For the chemistry simulation, the gas phase chemistry model used is the Regional Deposition Model version 2 (RADM2) (Stockwell et al. 1990), and the aerosol module includes the Modal Aerosol Dynamics for Europe (MADE) (Ackermann et al. 1998) and the Secondary Organic Aerosol Model (SORGAM) (Schell et al. 2001). The anthropogenic emissions of CO, NOx, SO₂, NH₃, BC, OC, PM_{2.5}, PM₁₀, and volatile organic compounds (VOC) are set based on the Multi-resolution Emission Inventory of China (MEIC) (<http://www.meicmodel.org>). The MEIC emission inventory contains the monthly anthropogenic emissions of five sectors: power, industry, residential, traffic, and agriculture. The emissions of September 2010 with the finest resolution of 0.25 °×0.25 ° is used in this study. To consider the diurnal variation of anthropogenic emissions, the diurnal variation information derived from the studies of Wang et al. (2010) and Olivier et al. (2003) is employed to generate the hourly anthropogenic emissions. In addition, to consider the vertical distribution of anthropogenic emissions, the emissions of power generators are set by using the vertical profiles of Wang et al. (2010), while the anthropogenic emissions of other sectors (i.e., agriculture, industry, traffic, residential) are only set at the lowest model layer. Although such emission

Fig. 2 The **a** ERA-interim and **b** simulated sea level pressure fields (hPa) at 0800 LT on 23 September 2011



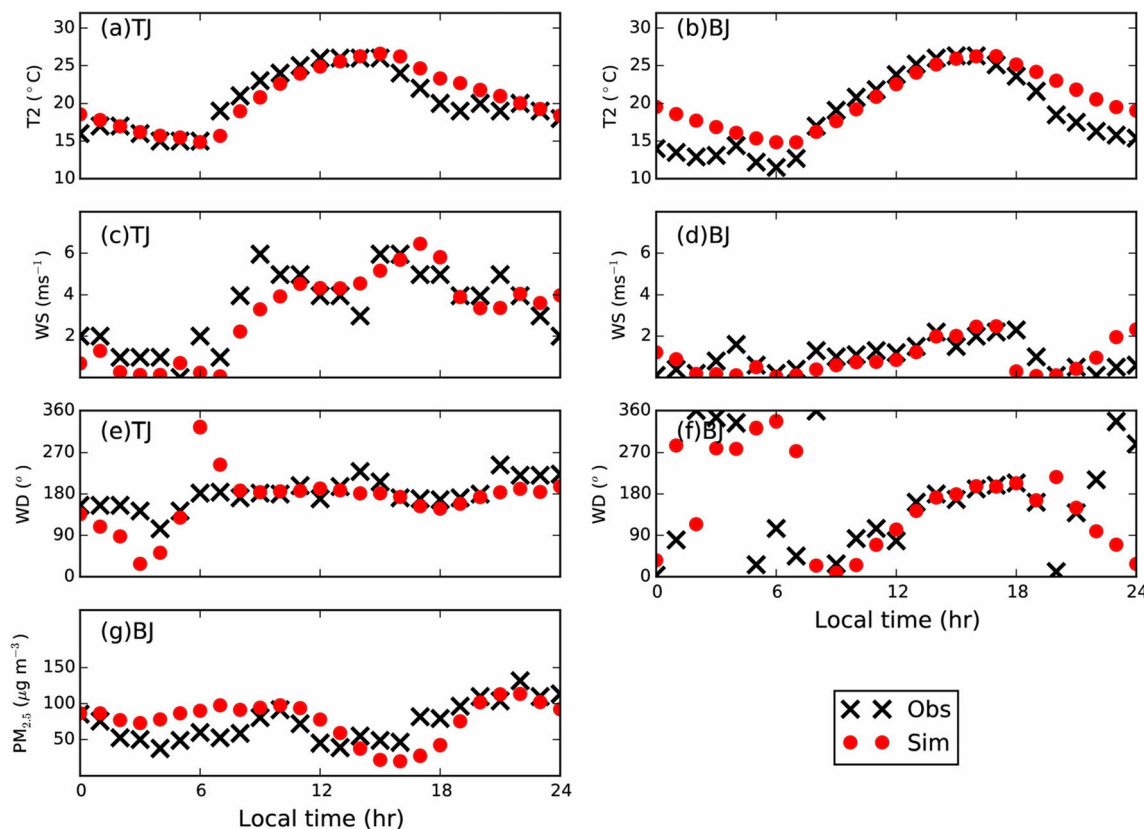


Fig. 3 The observed and simulated time series of (top to bottom) 2-m temperature (T_2), 10-m wind speed (WS), 10-m wind direction (WD), and $PM_{2.5}$ concentration on 23 September 2011 in Tianjin (TJ) (a, c, e) and

Beijing (BJ) (b, d, f, g). The $PM_{2.5}$ concentration was measured at ~20 m AGL, and the simulated $PM_{2.5}$ concentration was interpolated to the same height

configurations have some inherent uncertainties, they represent an improvement over the default setting of MEIC emissions (i.e., pollutants are emitted with a constant rate at a single model layer). Similar configurations of anthropogenic emissions had been used by Gao et al. (2015) to study the feedback between aerosol and meteorological variables in winter, and also by Zhang et al. (2015b) to investigate the effects of metrological anomalies on haze in Beijing.

In addition to the anthropogenic emissions, other emissions (i.e., biomass burning, biogenic, sea salt, and dust) are also included online into the model runs for this study: daily 1 km \times 1 km biomass burning emissions through the Fire Inventory from NCAR version-1.5 (FINNV1.5) (Wiedinmyer et al. 2011), as well as biogenic (Guenther et al. 1993, 1994), dust (Shaw et al. 2008), and sea salt emissions (Gong et al. 1997).

The initial and boundary conditions are set by the 6-hourly $1^\circ \times 1^\circ$ National Center for Environment Prediction (NCEP) global Final (FNL) reanalysis and the 6-hourly $1.9^\circ \times 2.5^\circ$ global analysis of Model for Ozone and Related chemical Tracers (MOZART) (<https://www2.acd.ucar.edu/wrf-chem/wrf-chem-tools-community>).

In this study, three independent 66-h WRF-Chem simulations are conducted from 0000 UTC (0800 local time (LT)) 21

September to 1800 UTC 23 September 2011, including a 40-h spin-up period. The simulation with the activated aerosol radiation option is regarded as the control run (hereafter referred as CTL), and a sensitive simulation without the aerosol radiation effect is regarded as the experimental run (EXP). In addition, to investigate the regional transport of pollutants, a blank sensitive simulation (BLK) is set by using the zero-out method (Streets et al. 2007; Zhang et al. 2015b) to set all

Table 1 The correlation coefficient (R), mean bias (MB), and root mean square error (RMSE) of meteorological and $PM_{2.5}$ simulations on 23 September 2011 at the Beijing (BJ) and Tianjin (TJ) sites

Variable	Site	R	MB	RMSE
T_2 (°C)	BJ	0.89 ^a	1.8	2.9
	TJ	0.89 ^a	0.4	1.8
WS (m s ⁻¹)	BJ	0.50 ^b	-0.1	0.7
	TJ	0.86 ^a	-0.4	1.1
WD (°)	BJ	0.64 ^a	-13.6	80.0
	TJ	0.53 ^b	-29.0	59.3
$PM_{2.5}$ (µg m ⁻³)	BJ	0.50 ^b	5.5	26.9

^a Confidence level, $p < 0.001$

^b Confidence level, $p < 0.02$

Fig. 4 The observed and simulated profiles of **a, b** potential temperature (*PT*); **c, d** mixing ration (*MR*); and **e, f** wind speed (*WS*) at 0800 and 2000 LT on 23 September 2011 at the Nanjiao sounding site in Beijing

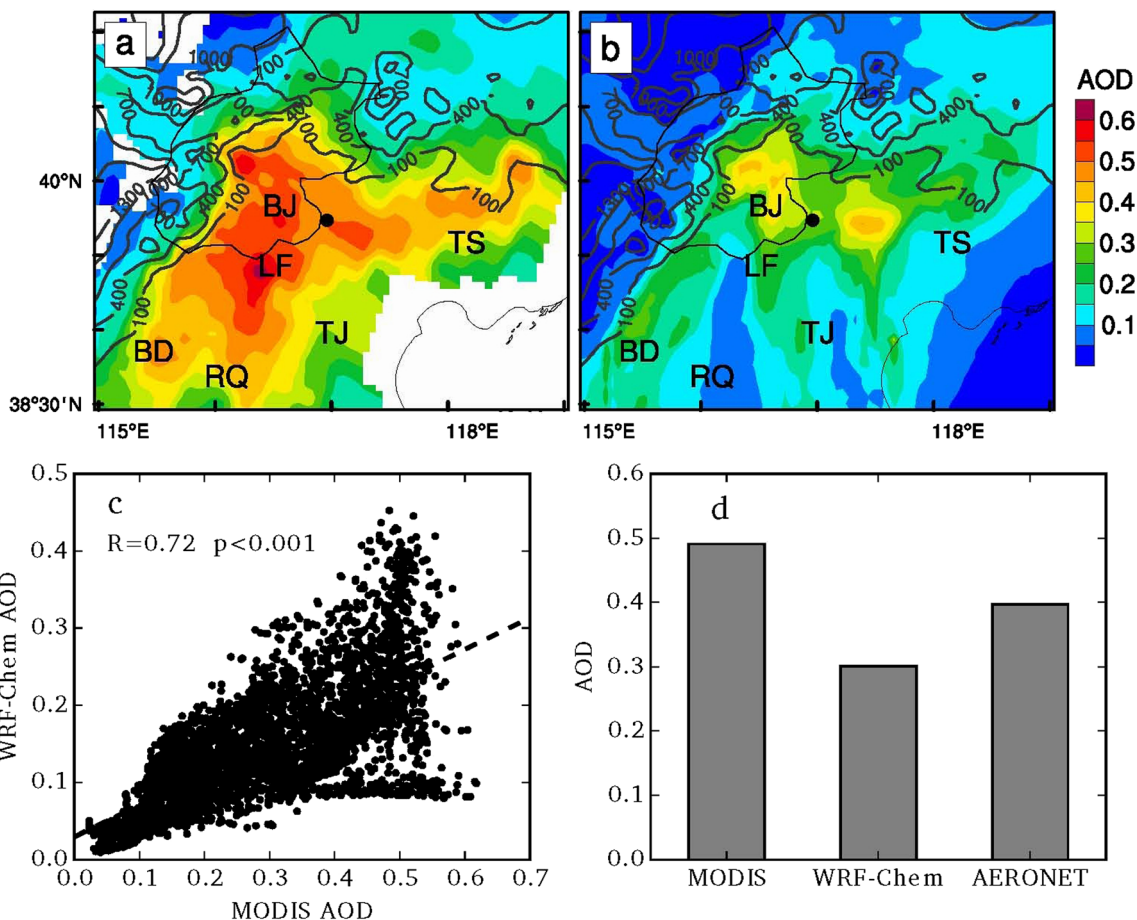
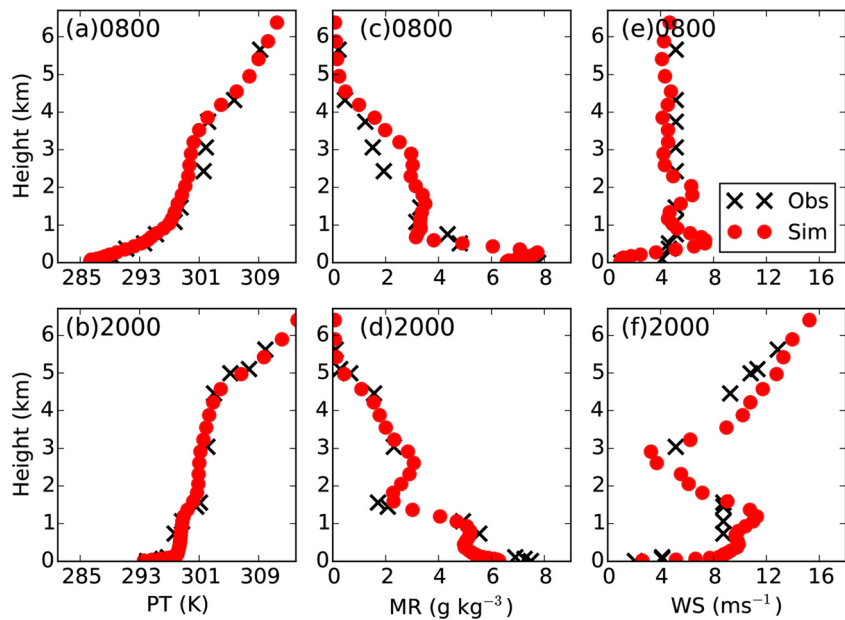


Fig. 5 The spatial distributions of **a** MODIS and **b** simulated aerosol optical depth (AOD) at ~1130 LT on 23 September 2011 overlaid with the contour lines of terrain height (m). **c** The scatter plot of MODIS AOD and simulated AOD. **d** The bar plot of MODIS AOD, simulated AOD, and AERONET AOD at ~1130 LT at the Xianghe site. **a, b** The location of

Xianghe site is marked by the *black dots* and the locations of Beijing (*BJ*), Tianjin (*TJ*), Tangshan (*TS*), Baoding (*BD*), Langfang (*LF*), and Renqiu (*RQ*) are marked by the *black texts*. **c** Note that to compare the MODIS AOD with the simulated AOD, the MODIS AOD is first interpolated to the WRF-Chem grids

anthropogenic emissions in Beijing to zero. Since the local circulations and the development of BL are driven by solar radiation, we focus on analyzing the aerosol radiation effect in the daytime in this study.

Data for simulation evaluation

The sea level pressure derived from the $0.75^\circ \times 0.75^\circ$ ERA-interim reanalysis (Dee et al. 2011) is used to analyze the synoptic condition and compare with the simulation (Fig. 2). The meteorological observations from two surface stations in

Beijing (40.02° N, 116.33° E) and Tianjin (39.12° N, 117.35° E) (marked by the red dots in Fig. 1b) are used to evaluate the simulations. The Beijing site, located on the urban area, is an Auto Weather Station deployed by the China Meteorological Administration (CMA) (Yang et al. 2013). The Tianjin site, located on the Tianjin Binhai International airport, is deployed by the Air Traffic Management Bureau of China; its observations are obtained from <http://www.wunderground.com>.

Besides the surface meteorological observations, the radiosonde sounding observations at the Nanjiao site (39.8° N, 116.467° E) in Beijing (marked by the triangle in

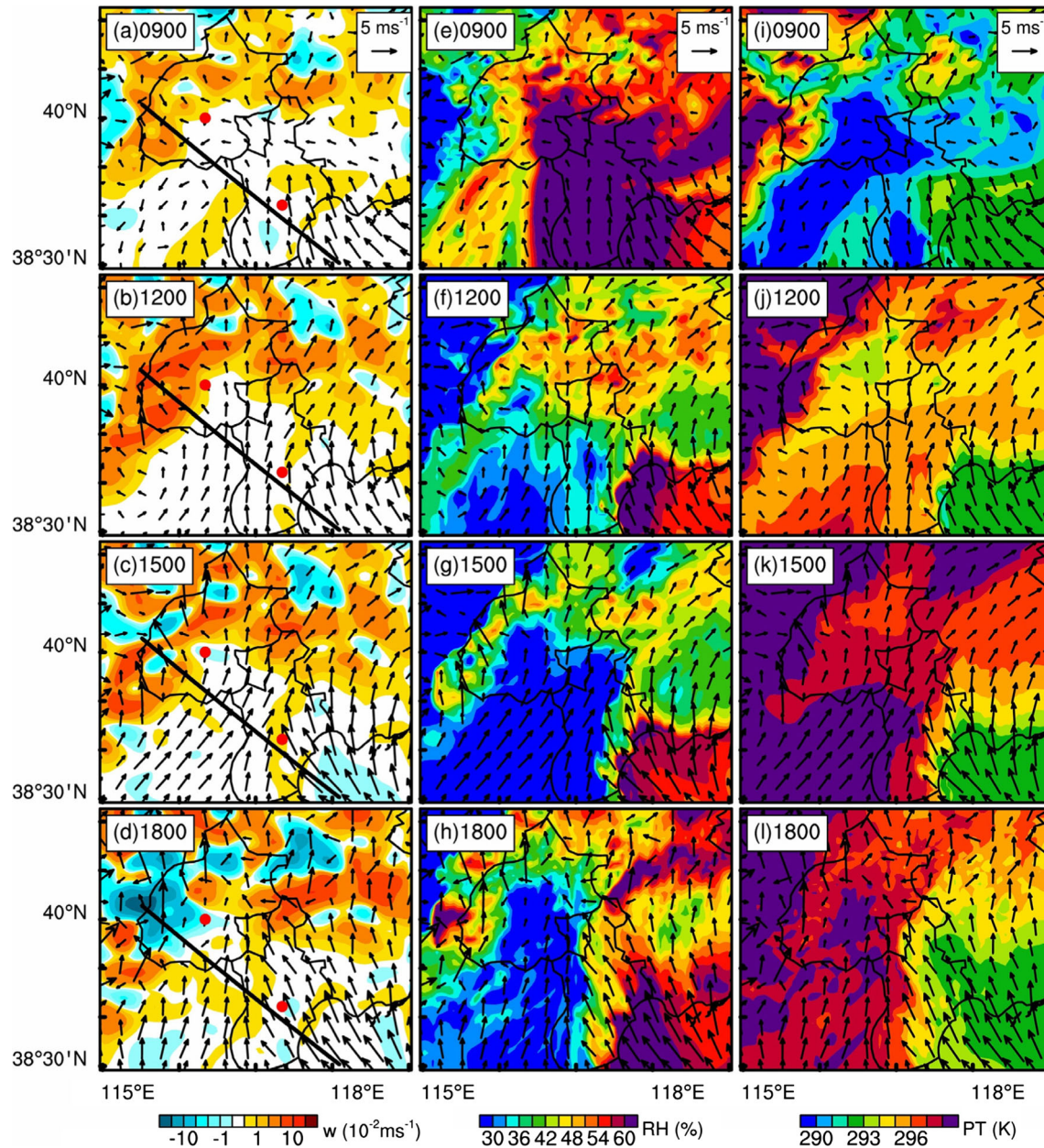


Fig. 6 The spatial distributions of **a–d** vertical velocity (w), **e–h** relative humidity (RH), and **i–l** potential temperature (PT) of CTL experiment at the second vertical layer (~ 35 m AGL), overlaid with 10-m wind vector fields at (top to bottom) 0900, 1200, 1500, and 1800 LT on 23 September 2011. **e–h** The red dots in (indicate the locations of two meteorological stations in Beijing and Tianjin and the black line indicates the locations of vertical cross sections shown in Figs. 8, 10, 12, and 17

2011. **e–h** The red dots in (indicate the locations of two meteorological stations in Beijing and Tianjin and the black line indicates the locations of vertical cross sections shown in Figs. 8, 10, 12, and 17

Fig. 7 The time series of observed **a** 2-m temperature (T_2 , shown by black lines) and its tendency (difference between current hour and previous hour, shown by blue bars) and **b** 2-m relative humidity (RH) and its tendency in Tianjin on 23 September 2011. The red bar indicates the passage of sea-breeze front (SBF)

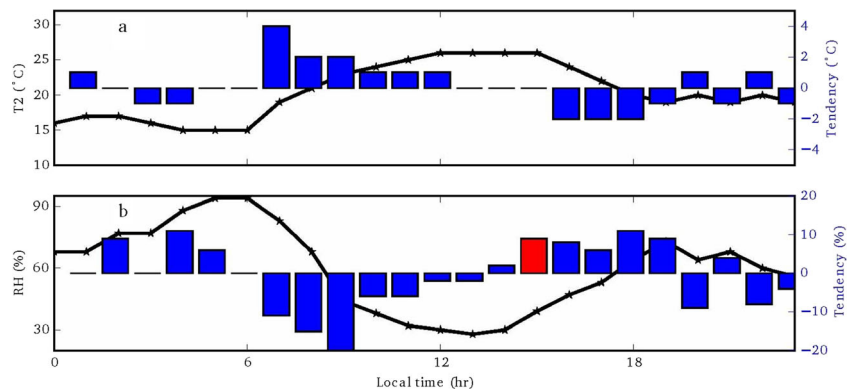


Fig. 1b) are also used to evaluate the simulations, which are obtained from <http://weather.uwyo.edu/upperair/sounding.html>.

In addition, the near-surface $PM_{2.5}$ concentration monitored at an urban station ($39.98^\circ N, 116.35^\circ E$, marked by the blue dot in Fig. 1b), the aerosol optical depth (AOD) measured at Xianghe site ($116.96^\circ N, 39.75^\circ E$, marked by the black dot in Fig. 1b) of the Aerosol Robotic Network (ARONET) (Holben et al. 1998), and the $10\text{ km} \times 10\text{ km}$ MODIS aerosol product (Sayer et al. 2014) are also used to evaluate the WRF-Chem simulations. The concentration of $PM_{2.5}$ was measured by the tapered element oscillating microbalance (Liu et al. 2013), and the AOD of Xianghe site was measured by the ground-based sun photometer (Cesnulyte et al. 2014). For the MODIS aerosol product, the “Deep_Blue_Aerosol_Optical_Depth_550_Land_Best_Estimate” dataset (Sayer et al. 2014) is used. In the WRF model, the aerosol optical properties are calculated based upon exact shell approximation (aer_op_opt=5), and the simulated AOD is calculated by integrating the simulated extinction coefficient from the surface to the atmospheric top.

Results

In this section, the simulations of WRF-Chem (CTL run) are first validated against the observations. Then, how the BL processes modulate the aerosol pollution in Beijing is presented, followed by the possible feedback between aerosol and BL processes.

Evaluation of the control run

During this pollution episode, a high pressure system is located to the east of Beijing (Fig. 2a), which supported a south-easterly near-surface synoptic wind to the BTH region and favored the development of local atmospheric circulations. Such synoptic condition is well reproduced by the model (Fig. 2b).

The diurnal variation evolution of mountain-plain breeze in Beijing could be observed from the measurements of wind direction (Fig. 3f), with the southerly upslope wind in the afternoon and the reversed downslope wind during nighttime. On the coastal areas, influenced by the onshore prevailing

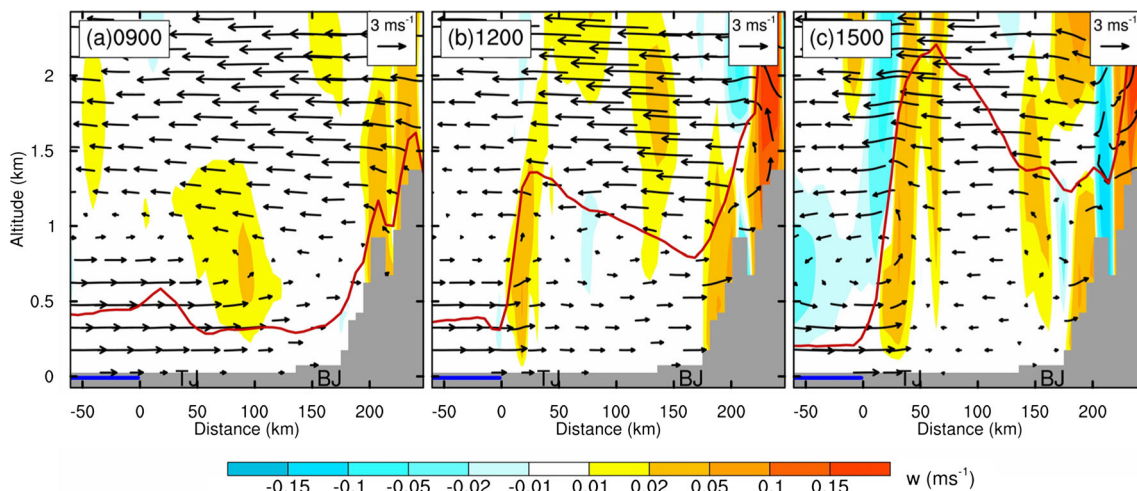


Fig. 8 The vertical cross sections of wind field of CTL experiment at **a** 0900 LT, **b** 1200 LT, and **c** 1500 LT on 23 September 2011. The location of cross section is marked in Fig. 6a. The red line represents the top of BL.

The blue line indicates the location of Bohai sea, and the locations of Beijing (BJ) and Tianjin (TJ) are indicated by the black texts. Note that the vertical velocity is multiplied by a factor of 20 when plotting wind vectors

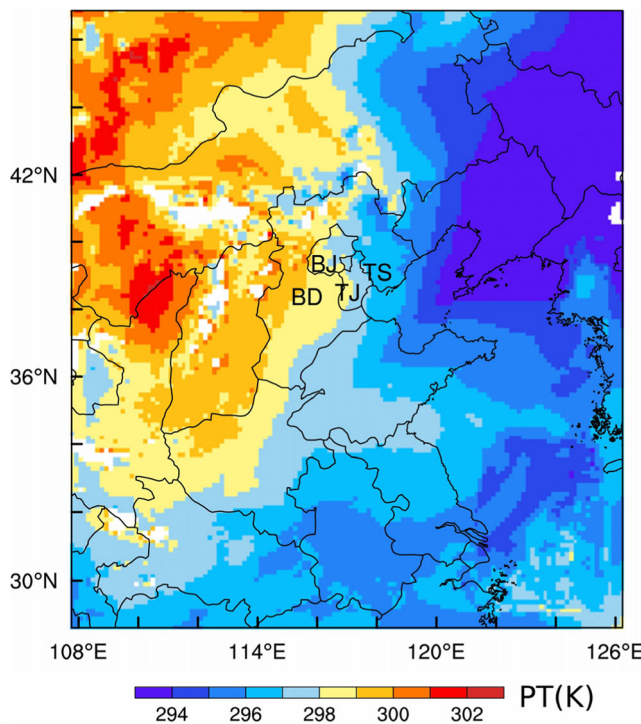


Fig. 9 The potential temperature (PT) at 1500-m altitude at 0900 LT on 23 September 2011 in domain 1. The locations of Beijing (*BJ*), Tianjin (*TJ*), Tangshan (*TS*), and Baoding (*BD*) are marked by the *black texts*

wind and the sea-breeze, it was the southerly onshore wind dominating in Tianjin during the whole day (Fig. 3e). From Fig. 3e, f and Table 1, it is found that these diurnal variations of wind direction in Beijing and Tianjin are well simulated by the model ($R=0.64$ and 0.53 , and mean bias (MB) $=-13.6^\circ$ and -29° at these two sites).

Figure 3a–d and Table 1 document a good model performance of the diurnal evolutions of 2-m temperature and 10-m wind speed in Beijing and Tianjin, although the model slightly overestimates the temperature (MB $=1.8$ and 0.4°C) and

under-predicts the wind speed (MB $=-0.1$ and -0.4 m s^{-1}) at these two sites.

In addition, as illustrated in Fig. 3g, the diurnal evolution of $\text{PM}_{2.5}$ in Beijing is also well reproduced by the model ($R=0.50$, MB $=5.5 \mu\text{g m}^{-3}$) (Table 1), with peak value occurring at around 2300 LT and minimum value in the afternoon. However, the model slightly overestimates the $\text{PM}_{2.5}$ concentration in the early morning from 0300 to 0800 LT and underestimates the $\text{PM}_{2.5}$ concentration in the afternoon from 1500 to 1800 LT. Such discrepancies between the simulated and observed $\text{PM}_{2.5}$ concentrations may be caused by the uncertainty of diurnal variation and vertical distribution of anthropogenic emissions.

The observed and simulated vertical profiles of potential temperature, mixing ratio, and wind speed at 0800 and 2000 LT on 23 September 2011 at the Nanjiao site are presented in Fig. 4. The vertical thermal and moisture profiles are well reproduced by the model (Fig. 4a–d). In addition, the general vertical structure of wind speed is also well simulated by the model (Fig. 4e–f), although the model overestimates the wind speed at some heights at 2000 LT.

The spatial distribution of MODIS AOD and simulated AOD at ~ 1130 LT is presented in Fig. 5a, b. Higher MODIS AOD is found in the plain areas adjacent to the Taihang Mountains and Yan Mountains (Fig. 5a), such as in Beijing, Langfang, and Baoding, while the relatively low AOD is found in the coastal areas (i.e., Tianjin and Tangshan). This spatial distribution of AOD indicates that the local atmospheric circulations may play a role in the transport of aerosols. Although the simulated AOD is generally lower than that of MODIS (Fig. 5b), the spatial variation of MODIS AOD is well reproduced by the model ($R=0.72$, Fig. 5c), with the higher AOD in the plains adjacent to the mountains. There is a north-to-south gap with a relatively low AOD in the simulated AOD field between Langfang and Renqiu (Fig. 5b),

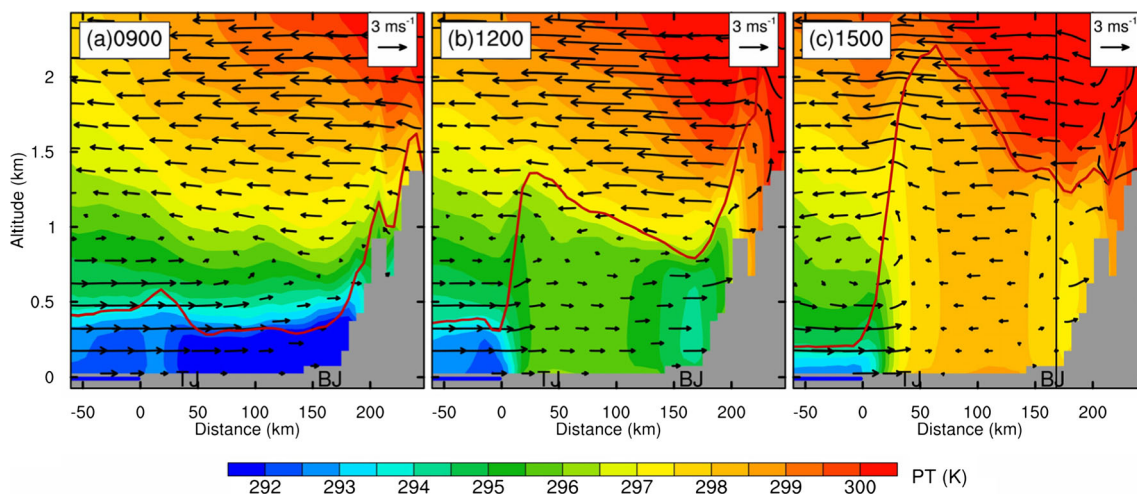
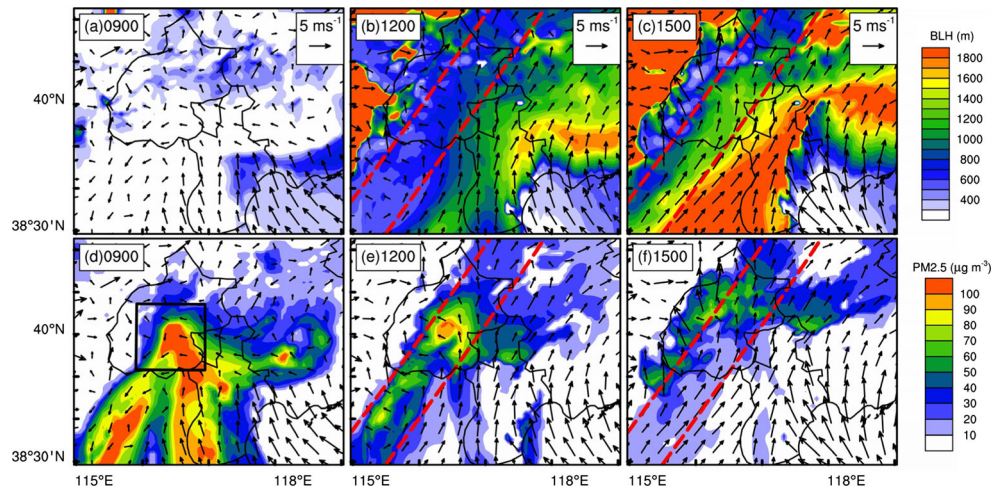


Fig. 10 Similar to Fig. 8, but for the vertical cross sections of potential temperature (PT) of CTL experiment at **a** 0900 LT, **b** 1200 LT, and **c** 1500 LT on 23 September 2011. **c** The *black line* in indicates the location where the PT profile is shown in Fig. 13

Fig. 11 The spatial distributions of **a–c** boundary layer height (BLH) and **d–f** surface PM_{2.5} concentration (the lowest vertical layer, ~10 m AGL) of CTL experiment overlaid with 10-m wind vector fields at (*left to right*) 0900, 1200, and 1500 LT on 23 September 2011. **b, c, f** The red dashed lines indicate the zone with relatively low BLH in the afternoon. **d** The black square indicates the sampling region of Beijing to plot Fig. 14



indicating that the emission of aerosols in this region may be underestimated. Besides, it should be noted that there are some inherent uncertainties related to the calculation of the aerosol optical properties in the model (Curci et al. 2015), such as the assumptions of mixing state, hygroscopicity, and refractive index.

Comparing the MODIS AOD and simulated AOD with the ground-based measured AOD at the Xianghe site (Fig. 5d), it

is found that the model tends to underestimate the AOD, while the MODIS AOD tends to overestimate it. Such discrepancies may be caused by the uncertainty of anthropogenic emissions (Kumar et al. 2014), uncertainties of simulated aerosol optical properties (Curci et al. 2015), and the uncertainty of MODIS retrieval algorithm (Li et al. 2009; Gao et al. 2015).

In general, the good model performance in terms of simulating the background synoptic forcing, near-surface wind,

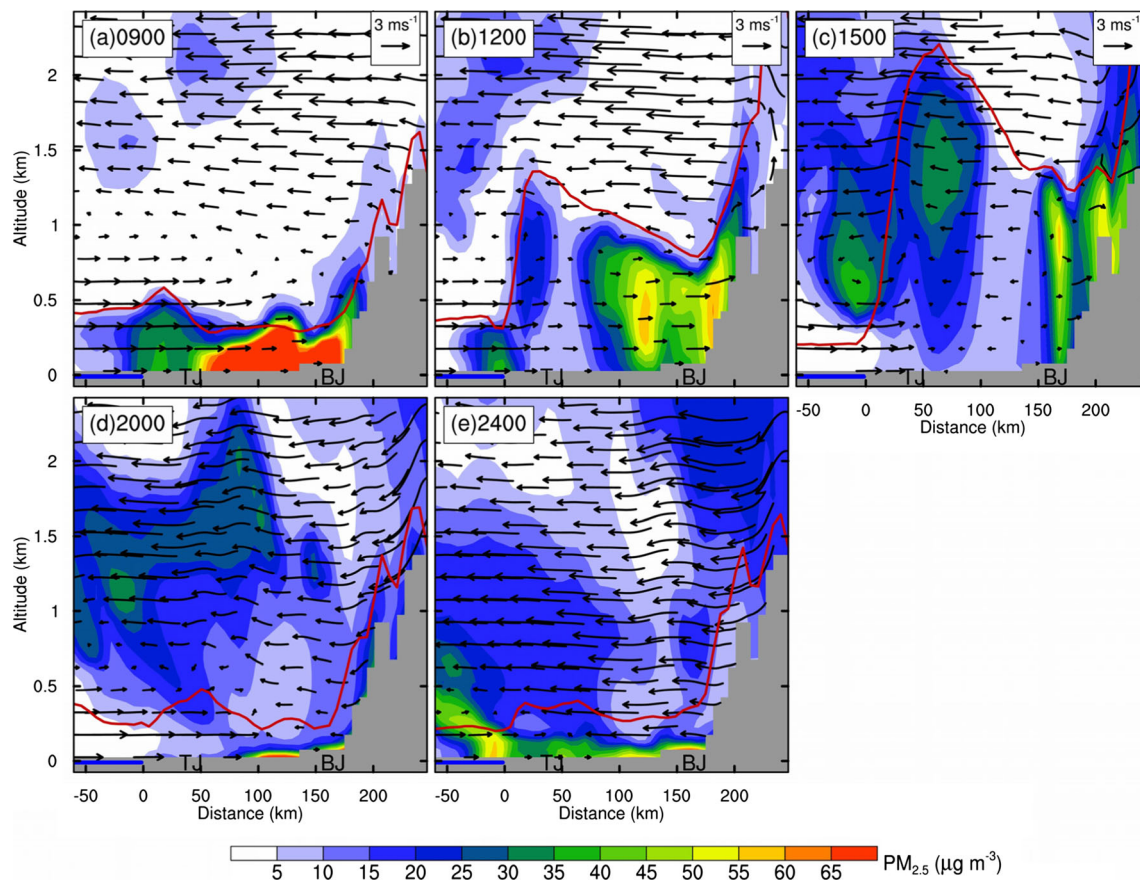


Fig. 12 Similar to Fig. 8, but for the vertical cross sections of PM_{2.5} concentration of CTL experiment at **a** 0900 LT, **b** 1200 LT, **c** 1500 LT, **d** 2000 LT, and **e** 2400 LT on 23 September 2011

temperature, $\text{PM}_{2.5}$ concentration, vertical profiles of atmosphere, and AOD spatial variation confirms the reliability of the model results on feedback between aerosol and local atmospheric circulation.

Effects of local circulations on aerosol pollution

As depicted in Fig. 3e, the southerly onshore wind dominates the coastal area during the whole day due to the background synoptic forcing (Fig. 2). Even in the morning when the land is still cooler than the sea (Fig. 6i) due to the synoptic forcing, the coastal areas are dominated by the onshore wind (Fig. 6a, e, i).

The onset of sea-breeze begins around 1100 LT in the coastal areas, induced by the thermal contrast between the land (warm) and sea (cool). At 1200 LT, a convergence belt with strong upward motion could be found in the coastal areas (Fig. 6b), which is the leading edge of sea-breeze, also named the sea-breeze front (SBF). The SBF is usually associated with sharp changes in temperature and moisture (Fig. 6f, j), with moister and cooler marine air behind it (Miller 2003). At 1500 LT, as the onshore synoptic forcing and the thermal difference between the land and sea persist, the SBF has penetrated inland ~ 50 km (Fig. 6c, g, k) and moved through the Tianjin area. The passage of SBF was observed at the surface observations (Fig. 7a, b) as an abrupt increase of relative humidity and decrease of temperature at around 1500 LT at the Tianjin site. At 1800 LT, the SBF has proceeded ~ 150 km from the coastal areas and reached the southeastern boundary of Beijing (Fig. 6d, h, l), and kept penetrating inland to the urban area of Beijing in the early evening.

The development and inland penetration of the sea-breeze are further illustrated in the vertical cross section of wind across the SBF (Fig. 8). At 1200 LT, a complete sea-breeze circulation cell is formed over the coastal area (Fig. 8b), constituted by the onshore flow and the offshore return flow aloft.

In addition to the development of sea-breeze, the mountain-plain breeze is also well established over the Beijing area. During daytime, as the mountain areas are warmed by the solar radiation, the air temperature adjacent to the mountains is higher than that of ambient air at the same altitude over the plains (Fig. 9). Such thermal contrast causes the upslope breeze starting around 0900 LT (Fig. 8a). And the upslope breeze becomes stronger in the afternoon (Fig. 8b, c), accompanied by a compensatory flow that is blown from the mountains to the adjacent plains aloft. In the afternoon, as the compensatory flow brings warmer air from the mountain areas to the adjacent plains, a relatively low thermal stable layer (with a higher potential temperature than that of BL) is formed above the BL over the Beijing area (Fig. 10b, c), which suppresses the development of BL there. As a result, the BLH over the plain areas adjacent to the Taihang Mountains and Yan Mountains is lower than that of rest plain areas, which is

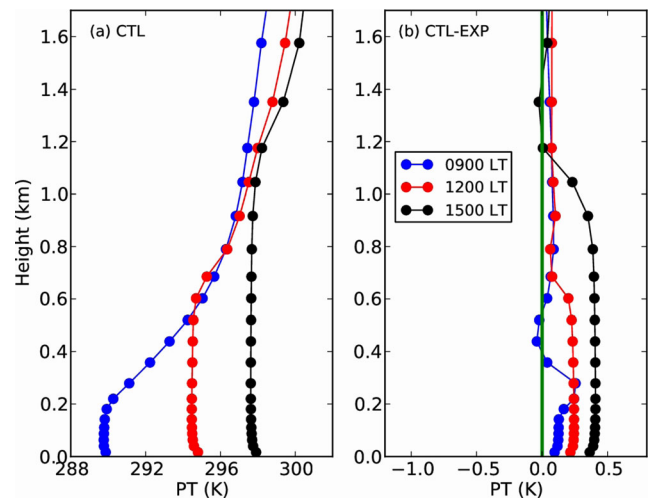


Fig. 13 **a** The potential temperature (PT) profiles in Beijing of the CTL run, and **b** the change ($CTL-EXP$) due to the aerosol radiation effect. The sampling location is marked in Fig. 10c by the black line

merely ~ 1.3 km at 1500 LT (Figs. 10c, 11c). This relatively low BLH may play a role in exacerbating the aerosol pollution there.

The spatial distribution of $\text{PM}_{2.5}$ is presented in Figs. 11 and 12, which is strongly influenced by the development of BL and the local atmospheric circulations. In the early morning, before the convective BL fully develops (Fig. 12a), the BLH over the most of BTH region is merely ~ 300 m (Figs. 11a, 12a). The vertical dispersion of aerosols is limited, and most aerosols are trapped within the shallow BL (Fig. 12a), resulting into a high near-surface concentration (Fig. 11d). Meanwhile, in presence of the onshore prevailing wind within the BL, the aerosols emitted from the coastal areas would be transported toward the mountain areas (Figs. 11d, 12a).

In the afternoon, in the vertical dimension as the convective BL grows (Fig. 13a) and the total dispersion volume increases, the surface aerosol concentration is decreased gradually (Fig. 11e, f). In the horizontal dimension, the presence of onshore sea-breeze facilitates the inland transport of aerosols (Fig. 11e). On the mountain side, the development of upslope

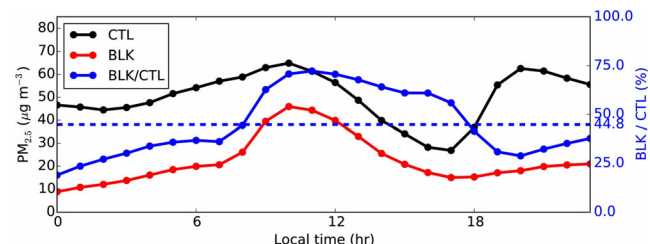


Fig. 14 Time series of surface $\text{PM}_{2.5}$ concentration of CTL experiment (black line) and BLK experiment (red line) averaged over Beijing on 23 September 2011, and the ratio between BLK and CTL experiments (blue line). The blue dashed line indicates the daily averaged ratio between the BLK and CTL experiments. The sampling region is marked in Fig. 11d by the black square

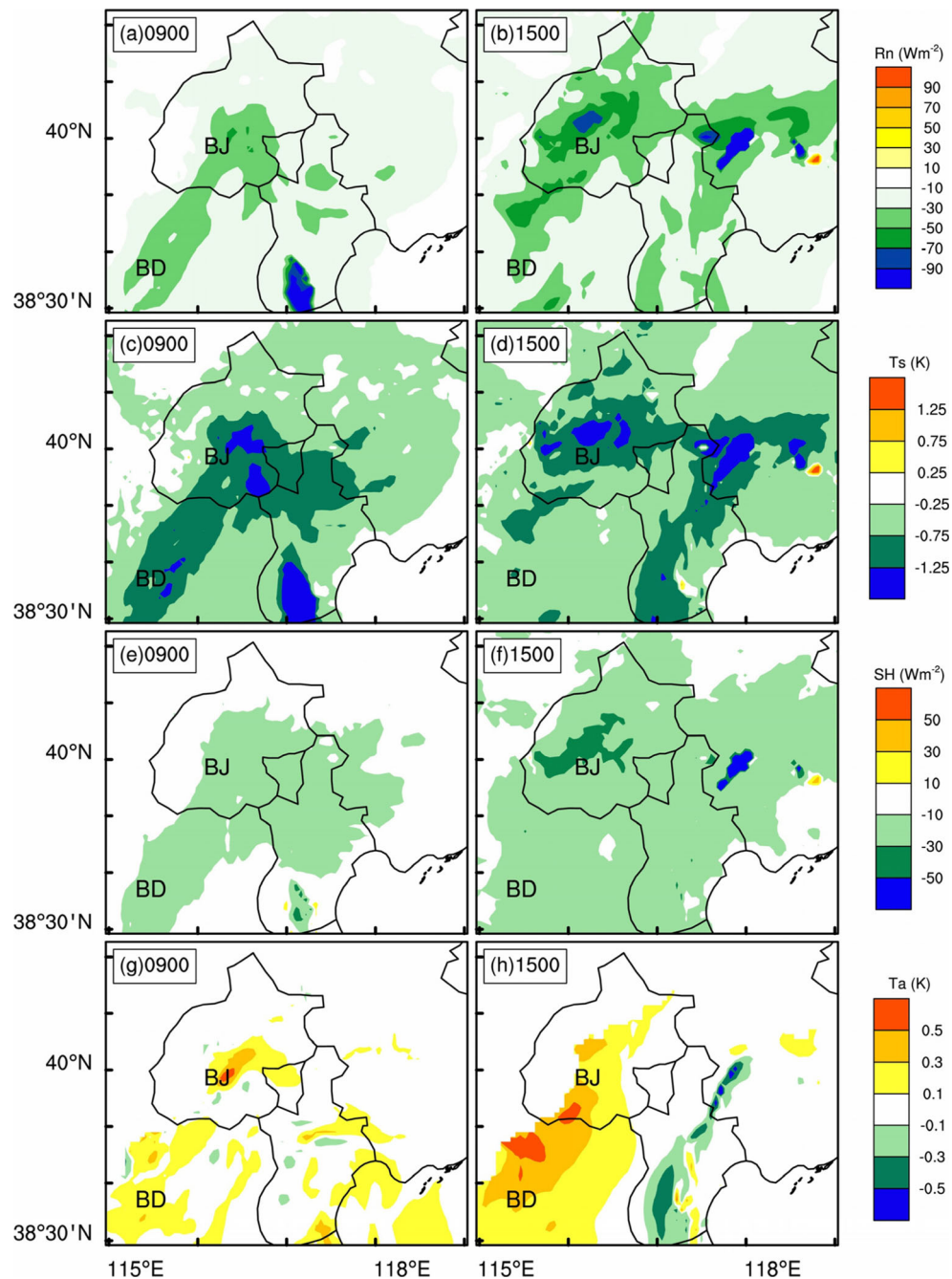
breeze also favors the horizontal transport of aerosols (Figs. 11e, f and 12b, c). As a result, most aerosols are accumulated over the plain areas adjacent to the Taihang Mountains and Yan Mountains (Fig. 11e, f).

After sunset, as the thermal contrast between the mountain and plain reverses, a downslope breeze occurs (Fig. 12d), which may drive the pollutants that have been carried away by the daytime upslope breeze back to the plain areas, and play a role in exacerbating the nighttime air quality (Fig. 12d–e). Such a day-to-night re-circulation of pollutants

had also been reported in the Lower Fraser Valley, Canada (Chow et al. 2012).

Comparing the surface-simulated PM_{2.5} concentrations of the CTL and BLK experiments, it is found that about 45 % of the simulated PM_{2.5} in Beijing are transported from other cities on 23 September 2011 (Fig. 14). The regional transport of aerosols to Beijing area is weak in the early morning and during the night. During the daytime, the development of sea-breeze and upslope breeze may play a role in facilitating the regional transport of aerosols (from the coastal areas to

Fig. 15 The changes (CTL-EXP) of **a, b** net radiation flux (Rn); **c, d** surface temperature (T_s); **e, f** surface sensible heat flux (SH); and **g, h** 950-hPa air temperature (T_a) due to aerosol radiation effect at (left to right) 0900 and 1500 LT on 23 September 2011. The locations of Beijing (BJ) and Baoding (BD) are marked by the black texts



Beijing). The contribution of regional transport peaks around 1100 LT (~60 % and $45 \mu\text{g m}^{-3}$), and decreases gradually afterwards. The decreases of regional contribution in the afternoon can be explained by the downward transport of tropospheric momentum. In the afternoon, as the convective BL fully develops, the offshore momentum is transported downward from the free troposphere to the surface layer (Fig. 8b, c), which may inhibit the regional transport of aerosols toward Beijing. Subsequently, in the evening, as the downslope breeze occurs, which is opposite to the onshore winds, the regional transport of aerosols is also suppressed.

Feedback between aerosol and BL processes

As the aerosols absorb and scatter the solar radiation, the surface net radiation flux is reduced by $10\text{--}50 \text{ W m}^{-2}$ during the daytime in the BTH region (Fig. 15a–b). Such reduction of radiation is more prominent in the western plain areas (i.e., Beijing and Baoding) along the mountains. The reduction of solar radiation reaching surface leads to the decrease of surface temperature and sensible heat flux in most of BTH region by $\sim 0.5\text{--}1 \text{ K}$ and $10\text{--}30 \text{ W m}^{-2}$, respectively (Fig. 15c–f). Meanwhile, the presence of aerosol increases air temperature within the BL by $0.1\text{--}0.5 \text{ K}$ (Figs. 13b, 15g, h), resulting into a more stable BL.

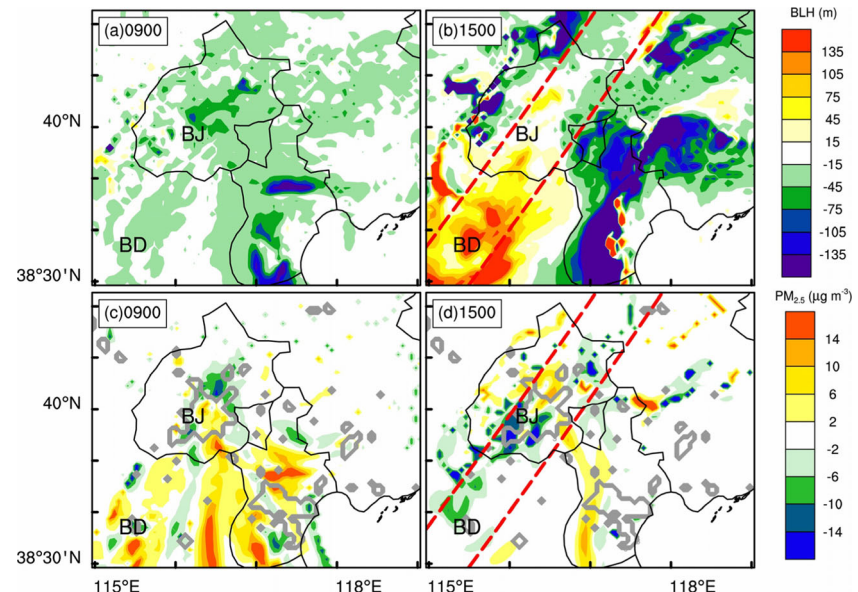
In the morning, due to the decrease of surface sensible heat flux and increase of BL stability, the turbulent mixing (for both vertical and horizontal dimensions) within the BL is suppressed. Therefore, the BLH is lowered by $\sim 10\text{--}30 \text{ m}$ (Figs. 16a, 17a), and the surface PM_{2.5} concentration is increased by $\sim 6 \mu\text{g m}^{-3}$ over the most of plain areas (Fig. 16c). In Beijing, it is found that more aerosols are likely to be accumulated over the urban area (Fig. 16c), while the

aerosol concentration is decreased in its rural areas due to the suppression of horizontal turbulent mixing. Such aerosol radiation feedback on the BLH and surface PM_{2.5} concentration has also been reported in previous studies (Quan et al. 2013; Wang et al. 2013; Gao et al. 2015).

Besides, the development of the local atmospheric circulations is also affected by the aerosol radiation effect, which brings out a different feedback between aerosol and BL processes. In the afternoon, as the aerosols are concentrated over the plain areas adjacent to the mountains, the BL air temperature there is increased by $0.1\text{--}0.5 \text{ K}$ (Figs. 13b, 15h, 17b), which decrease the thermal contrast between the mountains and its adjacent plain areas. As a result, the upslope breeze is weakened (Fig. 17d) and the presence of aerosols induced a downward motion over the mountain areas. Since in the afternoon, the presence of upslope breeze suppresses the growth of BL over the plain areas adjacent to the mountains (Figs. 10b, c and 11b, c), the weakening of upslope breeze may indirectly increase the BLH there (Figs. 16b, 17d), and decreases the surface PM_{2.5} concentration (Figs. 16d, 17f). Such a feedback exists in the western plain areas of the BTH region, where the distribution of aerosols is strongly influenced by the upslope breeze in the afternoon.

In the coastal areas, as the surface aerosols are lifted up to the BL top by the sea-breeze circulation in the afternoon (Fig. 12c), the air temperature at $\sim 2 \text{ km AGL}$ is warmed by the aerosol radiation effect (Fig. 17b). This warming effect increases the atmospheric stability, decreases the BLH, and suppresses the vertical exchange of momentum between the BL (onshore wind) and free troposphere (offshore wind) there. As a result, an onshore wind component is induced within the BL (Fig. 17d), and the aerosols are transported further inland to the northwest of Tianjin in the CTL experiment (Fig. 17f).

Fig. 16 The changes (CTL-EXP) of **a, b** boundary layer height (BLH) and **c, d** surface PM_{2.5} concentration due to aerosol radiation effect at (left to right) 0900 and 1500 LT on 23 September 2011. The red dashed lines in the right panel indicate the zone with relatively low BLH, and the urban areas are marked by the gray line (**c, d**). The locations of Beijing (BJ) and Baoding (BD) are marked by the black texts



Meanwhile, the induced onshore wind could bring more cool (wet) marine air to the Tianjin area, which may lead to a cooler BL there (Fig. 17b).

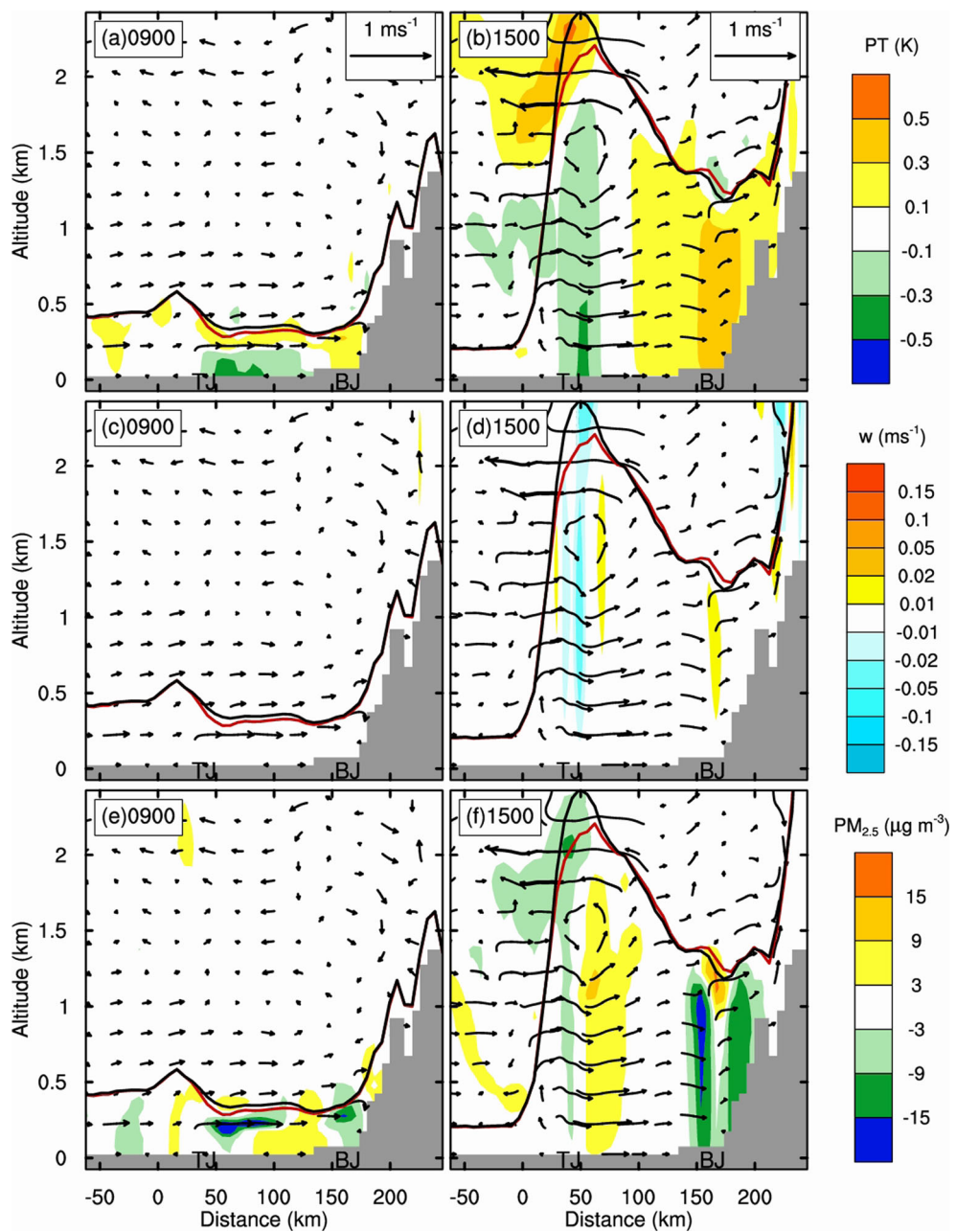
Conclusions

In this study, the effects of BL processes on aerosol pollution in Beijing and the feedback between the aerosol and BL processes are investigated by using the WRF-Chem. The first day of a haze episode which occurred on 23–27 September 2011 has been selected.

Fig. 17 The changes (CTL-EXP) of **a, b** potential temperature (PT); **c, d** vertical velocity; and **e, f** PM_{2.5} concentration due to the aerosol radiation effect at (*left to right*) 0900 and 1500 LT on 23 September 2011, overlaid with the changed field of wind vector. The locations of cross section are marked in Fig. 6a. The red and black lines indicate the BLH of CTL and EXP experiments, respectively. Note that the vertical velocity is multiplied by a factor of 20 when plotting wind vectors

It is found that the spatial distribution of aerosols is significantly modulated by the sea-land breeze and mountain-plain breeze. During the daytime, under the influence of sea-breeze, upslope breeze, and onshore prevailing wind, the aerosols emitted from the coastal areas could be transported to the downstream areas (i.e., Beijing and Baoding) and accumulated in the plain areas along the mountains.

In the afternoon, when the upslope breeze fully develops, its compensatory flow could bring the warmer air from the mountain areas to the adjacent plains (i.e., Beijing and Baoding), and form a relatively low thermal stable layer above the BL there. Such thermal stable layer suppresses the growth of BL and plays a role in exacerbating the aerosol pollution.



Two kinds of feedback between aerosol and BL processes during the daytime are found. As the aerosols absorb and scatter the solar radiation, the surface net radiation and sensible heat flux are decreased, while the BL air temperature is increased. As a result, the BL stability is increased and the BLH is lowered, which leads to higher surface PM_{2.5} concentration in the whole BTH region during the morning. The other kind of feedback is found in the adjacent plain areas (i.e., Beijing and Baoding) along the mountains in the afternoon. The presence of aerosols increases the BL air temperature over the plains, and the thermal contrast between the mountains and its adjacent plains driving the upslope breeze is weakened. As an indirect effect of this, the BL over the adjacent plains is heightened, and the surface PM_{2.5} concentration is decreased.

At last, through sensitive numerical experiments, it has been found that during this episode about 45 % of surface PM_{2.5} in Beijing are contributed by the regional transport. Therefore, to control the heavy aerosol pollution in Beijing, joint efforts to reduce emission among the cities in the whole BTH region are necessary.

Acknowledgments We thank Dr. Xiaoming Hu from University of Oklahoma for important advice. We thank Tsinghua University for providing the MEIC inventory. This work was supported by the National Sciences Foundation of China (Grant no. 41175004, 41465001), the China Meteorological Administration Special Public Welfare Research Fund (GYHY201106033), and the China Scholarship Council (CSC).

Compliance with ethical standards

Conflict of interest The authors declare that they have no competing interests.

References

- Ackermann IJ, Hass H, Memmesheimer M et al (1998) Modal aerosol dynamics model for Europe. *Atmos Environ* 32:2981–2999. doi:[10.1016/S1352-2310\(98\)00006-5](https://doi.org/10.1016/S1352-2310(98)00006-5)
- Albrecht BA (1989) Aerosols, cloud microphysics, and fractional cloudiness. *Science* 245(80-):1227–1230. doi:[10.1126/science.245.4923.1227](https://doi.org/10.1126/science.245.4923.1227)
- Atwater MA (1970) Planetary albedo changes due to aerosols. *Science* 170(80-):64–6. doi:[10.1126/science.170.3953.64](https://doi.org/10.1126/science.170.3953.64)
- Cesnulyte V, Lindfors a V, Pitkänen MR a et al (2014) Comparing ECMWF AOD with AERONET observations at visible and UV wavelengths. *Atmos Chem Phys* 14:593–608. doi:[10.5194/acp-14-593-2014](https://doi.org/10.5194/acp-14-593-2014)
- Chan CK, Yao X (2008) Air pollution in mega cities in China. *Atmos Environ* 42:1–42. doi:[10.1016/j.atmosenv.2007.09.003](https://doi.org/10.1016/j.atmosenv.2007.09.003)
- Che H, Xia X, Zhu J et al (2015) Aerosol optical properties under the condition of heavy haze over an urban site of Beijing, China. *Environ Sci Pollut Res Int* 22:1043–53. doi:[10.1007/s11356-014-3415-5](https://doi.org/10.1007/s11356-014-3415-5)
- Chen F, Dudhia J (2001) Coupling an advanced land surface–hydrology model with the Penn State–NCAR MM5 modeling system. Part II: preliminary model validation. *Mon Weather Rev* 129:587–604. doi:[10.1175/1520-0493\(2001\)129<0587:CAALSH>2.0.CO;2](https://doi.org/10.1175/1520-0493(2001)129<0587:CAALSH>2.0.CO;2)
- Chen Y, Zhao C, Zhang Q et al (2009) Aircraft study of mountain chimney effect of Beijing, China. *J Geophys Res Atmos* 114:1–10. doi:[10.1029/2008JD010610](https://doi.org/10.1029/2008JD010610)
- Chow FK, De Wekker SF, Snyder BJ (2012) Mountain weather research and forecasting: recent progress and current challenges. Springer Science & Business Media. doi:[10.1007/978-94-007-4098-3](https://doi.org/10.1007/978-94-007-4098-3)
- Coakley JA, Cess RD, Yurevich FB (1983) The effect of tropospheric aerosols on the Earth's radiation budget: a parameterization for climate models. *J Atmos Sci* 40:116–138. doi:[10.1175/1520-0469\(1983\)040<0116:TEOTAO>2.0.CO;2](https://doi.org/10.1175/1520-0469(1983)040<0116:TEOTAO>2.0.CO;2)
- Crosman ET, Horel JD (2010) Sea and lake breezes: a review of numerical studies. *Bound-Layer Meteorol* 137:1–29. doi:[10.1007/s10546-010-9517-9](https://doi.org/10.1007/s10546-010-9517-9)
- Curci G, Hogrefe C, Bianconi R et al (2015) Uncertainties of simulated aerosol optical properties induced by assumptions on aerosol physical and chemical properties: an AQMEII-2 perspective. *Atmos Environ* 115:541–552. doi:[10.1016/j.atmosenv.2014.09.009](https://doi.org/10.1016/j.atmosenv.2014.09.009)
- Dee DP, Uppala SM, Simmons AJ et al (2011) The ERA-Interim reanalysis: configuration and performance of the data assimilation system. *Q J R Meteorol Soc* 137:553–597. doi:[10.1002/qj.828](https://doi.org/10.1002/qj.828)
- Dou J, Wang Y, Bornstein R, Miao S (2015) Observed spatial characteristics of Beijing urban climate impacts on summer thunderstorms. *J Appl Meteorol Climatol* 54:94–105. doi:[10.1175/JAMC-D-13-0355.1](https://doi.org/10.1175/JAMC-D-13-0355.1)
- Fu GQ, Xu WY, Yang RF et al (2014) The distribution and trends of fog and haze in the North China Plain over the past 30 years. *Atmos Chem Phys* 14:11949–11958. doi:[10.5194/acp-14-11949-2014](https://doi.org/10.5194/acp-14-11949-2014)
- Gao Y, Zhang M, Liu Z et al (2015) Modeling the feedback between aerosol and meteorological variables in the atmospheric boundary layer during a severe fog–haze event over the North China Plain. *Atmos Chem Phys* 15:4279–4295. doi:[10.5194/acp-15-4279-2015](https://doi.org/10.5194/acp-15-4279-2015)
- Gong SL, Barrie LA, Blanchet J-P (1997) Modeling sea-salt aerosols in the atmosphere: 1. Model development. *J Geophys Res* 102:3805. doi:[10.1029/96JD02953](https://doi.org/10.1029/96JD02953)
- Grell GA, Freitas SR (2014) A scale and aerosol aware stochastic convective parameterization for weather and air quality modeling. *Atmos Chem Phys* 14:5233–5250. doi:[10.5194/acp-14-5233-2014](https://doi.org/10.5194/acp-14-5233-2014)
- Grell GA, Peckham SE, Schmitz R et al (2005) Fully coupled “online” chemistry within the WRF model. *Atmos Environ* 39:6957–6975. doi:[10.1016/j.atmosenv.2005.04.027](https://doi.org/10.1016/j.atmosenv.2005.04.027)
- Guenther A, Zimmerman P, Wildermuth M (1994) Natural volatile organic compound emission rate estimates for U.S. woodland landscapes. *Atmos Environ* 28:1197–1210. doi:[10.1016/1352-2310\(94\)90297-6](https://doi.org/10.1016/1352-2310(94)90297-6)
- Guenther AB, Zimmerman PR, Harley PC et al (1993) Isoprene and monoterpene emission rate variability: model evaluations and sensitivity analyses. *J Geophys Res* 98:12609. doi:[10.1029/93JD00527](https://doi.org/10.1029/93JD00527)
- Han T, Liu X, Zhang Y et al (2015) Role of secondary aerosols in haze formation in summer in the Megacity Beijing. *J Environ Sci* 31:51–60. doi:[10.1016/j.jes.2014.08.026](https://doi.org/10.1016/j.jes.2014.08.026)
- He K, Yang F, Ma Y et al (2001) The characteristics of PM_{2.5} in Beijing, China. *Atmos Environ* 35:4959–4970. doi:[10.1016/S1352-2310\(01\)00301-6](https://doi.org/10.1016/S1352-2310(01)00301-6)
- Holben BN, Eck TF, Slutsker I et al (1998) AERONET—a federated instrument network and data archive for aerosol characterization. *Remote Sens Environ* 66:1–16. doi:[10.1016/S0034-4257\(98\)00031-5](https://doi.org/10.1016/S0034-4257(98)00031-5)
- Hong S-Y, Noh Y, Dudhia J (2006) A New vertical diffusion package with an explicit treatment of entrainment processes. *Mon Weather Rev* 134:2318–2341. doi:[10.1175/MWR3199.1](https://doi.org/10.1175/MWR3199.1)
- Hu X, Ma Z, Lin W et al (2014) Impact of the Loess Plateau on the atmospheric boundary layer structure and air quality in the North China Plain: a case study. *Sci Total Environ* 499:228–237. doi:[10.1016/j.scitotenv.2014.08.053](https://doi.org/10.1016/j.scitotenv.2014.08.053)

- Huang R-J, Zhang Y, Bozzetti C et al (2014) High secondary aerosol contribution to particulate pollution during haze events in China. *Nature*. doi:[10.1038/nature13774](https://doi.org/10.1038/nature13774)
- Huang X, Song Y, Zhao C et al (2015) Direct radiative effect by multi-component aerosol over China*. *J Clim* 28:3472–3495. doi:[10.1175/JCLI-D-14-00365.1](https://doi.org/10.1175/JCLI-D-14-00365.1)
- Iacono MJ, Delamere JS, Mlawer EJ et al (2008) Radiative forcing by long-lived greenhouse gases: calculations with the AER radiative transfer models. *J Geophys Res* 113:D13103. doi:[10.1029/2008JD009944](https://doi.org/10.1029/2008JD009944)
- Justice C, Townshend JR, Vermote E et al (2002) An overview of MODIS Land data processing and product status. *Remote Sens Environ* 83: 3–15. doi:[10.1016/S0034-4257\(02\)00084-6](https://doi.org/10.1016/S0034-4257(02)00084-6)
- Kumar R, Barth MC, Pfister GG et al (2014) WRF-Chem simulations of a typical pre-monsoon dust storm in northern India: influences on aerosol optical properties and radiation budget. *Atmos Chem Phys* 14:2431–2446. doi:[10.5194/acp-14-2431-2014](https://doi.org/10.5194/acp-14-2431-2014)
- Kusaka H, Kondo H, Kikegawa Y, Kimura F (2001) A simple single-layer urban canopy model for atmospheric models: comparison with multi-layer and slab models. *Bound-Layer Meteorol* 101:329–358. doi:[10.1023/A:1019207923078](https://doi.org/10.1023/A:1019207923078)
- Li R, Li Z, Gao W et al (2014) Diurnal, seasonal, and spatial variation of PM2.5 in Beijing. *Sci Bull* 60:387–395. doi:[10.1007/s11434-014-0607-9](https://doi.org/10.1007/s11434-014-0607-9)
- Li Z, Xia X, Cribb M et al (2007) Aerosol optical properties and their radiative effects in northern China. *J Geophys Res* 112:1–11. doi:[10.1029/2006JD007382](https://doi.org/10.1029/2006JD007382)
- Li Z, Zhao X, Kahn R et al (2009) Uncertainties in satellite remote sensing of aerosols and impact on monitoring its long-term trend: a review and perspective. *Ann Geophys* 27:2755–2770. doi:[10.5194/angeo-27-2755-2009](https://doi.org/10.5194/angeo-27-2755-2009)
- Lin Y-L, Farley RD, Orville HD (1983) Bulk parameterization of the snow field in a cloud model. *J Clim Appl Meteorol* 22:1065–1092. doi:[10.1175/1520-0450\(1983\)022<1065:BPOTSF>2.0.CO;2](https://doi.org/10.1175/1520-0450(1983)022<1065:BPOTSF>2.0.CO;2)
- Liu H, Zhang L, Wu J (2010) A modeling study of the climate effects of sulfate and carbonaceous aerosols over China. *Adv Atmos Sci* 27: 1276–1288. doi:[10.1007/s00376-010-9188-y](https://doi.org/10.1007/s00376-010-9188-y)
- Liu J, Xia X, Wang P et al (2007) Significant aerosol direct radiative effects during a pollution episode in northern China. *Geophys Res Lett* 34:1–5. doi:[10.1029/2007GL030953](https://doi.org/10.1029/2007GL030953)
- Liu S, Liu Z, Li J et al (2009) Numerical simulation for the coupling effect of local atmospheric circulations over the area of Beijing, Tianjin and Hebei Province. *Sci China Ser D Earth Sci* 52:382–392. doi:[10.1007/s11430-009-0030-2](https://doi.org/10.1007/s11430-009-0030-2)
- Liu XG, Li J, Qu Y et al (2013) Formation and evolution mechanism of regional haze: a case study in the megacity Beijing, China. *Atmos Chem Phys* 13:4501–4514. doi:[10.5194/acp-13-4501-2013](https://doi.org/10.5194/acp-13-4501-2013)
- Miao Y, Liu S, Zheng Y et al (2015a) Numerical study of the effects of topography and urbanization on the local atmospheric circulations over the Beijing-Tianjin-Hebei, China. *Adv Meteorol* 2015:1–16. doi:[10.1155/2015/397070](https://doi.org/10.1155/2015/397070)
- Miao Y, Liu S, Zheng Y et al (2015b) Numerical study of the effects of local atmospheric circulations on a pollution event over Beijing-Tianjin-Hebei, China. *J Environ Sci* 30:9–20. doi:[10.1016/j.jes.2014.08.025](https://doi.org/10.1016/j.jes.2014.08.025)
- Miller STK (2003) Sea breeze: structure, forecasting, and impacts. *Rev Geophys* 41:1011. doi:[10.1029/2003RG000124](https://doi.org/10.1029/2003RG000124)
- Olivier J, Peters J, Granier C et al (2003) Present and future surface emissions of atmospheric compounds. POET Report #2, EU project EVK2-1999-00011
- Qian Y, Ruby Leung L, Ghan SJ, Giorgi F (2003) Regional climate effects of aerosols over China: modeling and observation. *Tellus B* 55:914–934. doi:[10.1046/j.1435-6935.2003.00070.x](https://doi.org/10.1046/j.1435-6935.2003.00070.x)
- Quan J, Gao Y, Zhang Q et al (2013) Evolution of planetary boundary layer under different weather conditions, and its impact on aerosol concentrations. *Particuology* 11:34–40. doi:[10.1016/j.partic.2012.04.005](https://doi.org/10.1016/j.partic.2012.04.005)
- Quan J, Tie X, Zhang Q et al (2014) Characteristics of heavy aerosol pollution during the 2012–2013 winter in Beijing, China. *Atmos Environ* 88:83–89. doi:[10.1016/j.atmosenv.2014.01.058](https://doi.org/10.1016/j.atmosenv.2014.01.058)
- Ramanathan V, Crutzen PJ, Kiehl JT, Rosenfeld D (2001) Aerosols, climate, and the hydrological cycle. *Science* 294(80):2119–24. doi:[10.1126/science.1064034](https://doi.org/10.1126/science.1064034)
- Rosenfeld D, Lensky IM (1998) Satellite-based insights into precipitation formation processes in continental and maritime convective clouds. *Bull Am Meteorol Soc* 79:2457–2476. doi:[10.1175/1520-0477\(1998\)079<2457:SBIIPF>2.0.CO;2](https://doi.org/10.1175/1520-0477(1998)079<2457:SBIIPF>2.0.CO;2)
- Saha A, Mallet M, Roger JC et al (2008) One year measurements of aerosol optical properties over an urban coastal site: Effect on local direct radiative forcing. *Atmos Res* 90:195–202. doi:[10.1016/j.atmosres.2008.02.003](https://doi.org/10.1016/j.atmosres.2008.02.003)
- San Martini FM, Hasenkopf CA, Roberts DC (2015) Statistical analysis of PM2.5 observations from diplomatic facilities in China. *Atmos Environ* 110:174–185. doi:[10.1016/j.atmosenv.2015.03.060](https://doi.org/10.1016/j.atmosenv.2015.03.060)
- Sayer AM, Munchak LA, Hsu NC et al (2014) MODIS collection 6 aerosol products: comparison between Aqua's e-deep blue, dark target, and "merged" data sets, and usage recommendations. *J Geophys Res Atmos* 119:13,965–13,989. doi:[10.1002/2014JD022453](https://doi.org/10.1002/2014JD022453)
- Schell B, Ackermann IJ, Hass H et al (2001) Modeling the formation of secondary organic aerosol within a comprehensive air quality model system. *J Geophys Res Atmos* 106:28275–28293. doi:[10.1029/2001JD000384](https://doi.org/10.1029/2001JD000384)
- Serafin S, Zardi D (2010) Daytime heat transfer processes related to slope flows and turbulent convection in an idealized mountain valley. *J Atmos Sci* 67:3739–3756. doi:[10.1175/2010JAS3428.1](https://doi.org/10.1175/2010JAS3428.1)
- Shaw WJ, Jerry Allwine K, Fritz BG et al (2008) An evaluation of the wind erosion module in DUSTTRAN. *Atmos Environ* 42:1907–1921. doi:[10.1016/j.atmosenv.2007.11.022](https://doi.org/10.1016/j.atmosenv.2007.11.022)
- Sokolik IN, Toon OB (1996) Direct radiative forcing by airborne mineral aerosols. *J Aerosol Sci* 27:S11–S12. doi:[10.1016/0021-8502\(96\)00078-X](https://doi.org/10.1016/0021-8502(96)00078-X)
- Stockwell WR, Middleton P, Chang JS, Tang X (1990) The second generation regional acid deposition model chemical mechanism for regional air quality modeling. *J Geophys Res* 95:16343. doi:[10.1029/JD095iD10p16343](https://doi.org/10.1029/JD095iD10p16343)
- Streets DG, Fu JS, Jang CJ et al (2007) Air quality during the 2008 Beijing olympic games. *Atmos Environ* 41:480–492. doi:[10.1016/j.atmosenv.2006.08.046](https://doi.org/10.1016/j.atmosenv.2006.08.046)
- Sun Y, Song T, Tang G, Wang Y (2013) The vertical distribution of PM2.5 and boundary-layer structure during summer haze in Beijing. *Atmos Environ* 74:413–421. doi:[10.1016/j.atmosenv.2013.03.011](https://doi.org/10.1016/j.atmosenv.2013.03.011)
- Wang X, Liang X, Jiang W et al (2010) WRF-Chem simulation of East Asian air quality: Sensitivity to temporal and vertical emissions distributions. *Atmos Environ* 44(5):660–669. doi:[10.1016/j.atmosenv.2009.11.011](https://doi.org/10.1016/j.atmosenv.2009.11.011)
- Wang J, Wang S, Jiang J, Ding A (2013) Impact of aerosol – meteorology interactions on fine particle pollution during China's severe haze episode in January 2013. *Environ Res Lett*. doi:[10.1088/1748-9326/9/9/094002](https://doi.org/10.1088/1748-9326/9/9/094002)
- Wiedinmyer C, Akagi SK, Yokelson RJ et al (2011) The Fire INVENTORY from NCAR (FINN): a high resolution global model to estimate the emissions from open burning. *Geosci Model Dev* 4:625–641. doi:[10.5194/gmd-4-625-2011](https://doi.org/10.5194/gmd-4-625-2011)
- Xia X, Li Z, Wang P et al (2007) Estimation of aerosol effects on surface irradiance based on measurements and radiative transfer model simulations in northern China. *J Geophys Res Atmos* 112:1–11. doi:[10.1029/2006JD008337](https://doi.org/10.1029/2006JD008337)

- Yang P, Ren G, Liu W (2013) Spatial and temporal characteristics of Beijing urban heat island intensity. *J Appl Meteorol Climatol* 52: 1803–1816. doi:[10.1175/JAMC-D-12-0125.1](https://doi.org/10.1175/JAMC-D-12-0125.1)
- Yu H, Kaufman YJ, Chin M et al (2006) A review of measurement-based assessments of the aerosol direct radiative effect and forcing. *Atmos Chem Phys* 6:613–666. doi:[10.5194/acp-6-613-2006](https://doi.org/10.5194/acp-6-613-2006)
- Zhang B, Wang Y, Hao J (2015a) Simulating aerosol–radiation–cloud feedbacks on meteorology and air quality over eastern China under severe haze conditions in winter. *Atmos Chem Phys* 15:2387–2404. doi:[10.5194/acp-15-2387-2015](https://doi.org/10.5194/acp-15-2387-2015)
- Zhang et al (2013) Numerical simulation of characteristics of summer clear day boundary layer in Beijing and the impact of urban underlying surface on sea breeze. *Chinese J Geophys Ed* 8:2558–2573. doi:[10.6038/cjg20130806](https://doi.org/10.6038/cjg20130806)
- Zhang L, Wang T, Lv M, Zhang Q (2015b) On the severe haze in Beijing during January 2013 : unraveling the effects of meteorological anomalies with WRF-chem. *Atmos Environ* 104:11–21. doi:[10.1016/j.atmosenv.2015.01.001](https://doi.org/10.1016/j.atmosenv.2015.01.001)
- Zhuang B, Jiang F, Wang T et al (2010) Investigation on the direct radiative effect of fossil fuel black-carbon aerosol over China. *Theor Appl Climatol* 104:301–312. doi:[10.1007/s00704-010-0341-4](https://doi.org/10.1007/s00704-010-0341-4)